Design Improvement of a New Outer-Rotor Hybrid Excitation Flux Switching Motor for In-Wheel Drive EV

[1]M. Z. Ahmad, [2] E. Sulaiman, and [3] Z. A. Haron
Dept. of Electrical Power Engineering
Faculty of Electrical & Electronic Engineering
Universiti Tun Hussein Onn Malaysia
Johor, Malaysia
[1]zarafi@uthm.edu.my, [2] erwan@uthm.edu.my,
[3]zainalal@uthm.edu.my

T. Kosaka
Dept. of Electrical and Computer Engineering
Nagoya Institute of Technology (NIT)
Nagoya, Japan
kosaka@nitech.ac.jp

Abstract — **Research and developments of in-wheel motors applied in pure electric vehicles (EVs) propulsion systems have attracted great attention recently. This is due to their definite advantages of great controllability for each independent wheel as well as the availability of more cabin space due to removal of conventional mechanical transmission and differential gears. Moreover, more series batteries can be installed to increase the driving distance. Since the motors are attached directly to the wheel, the major requirements are to have high torque density and efficiency. As one of alternative candidates with high torque possibility, a new design of outer-rotor hybrid excitation flux switching motor for in-wheel drive EV is proposed in this paper. The proposed motor consists of 12 slots of stator poles, and 10 rotor poles, with all active parts are located on the stator. In addition, it has a robust rotor structure which only comprises a single piece of rotor and has a wide range flux control capabilities. Under some design restrictions and specifications for the target EV drive applications, the performance of the proposed machine on the initial design and improved design are analyzed based on 2-D finite element analysis (FEA). The performance of the improved design motor shows that the maximum torque achieved is 81.5% of the target performance, whereas the maximum power has achieved 143.6 kW which is greater than the target value. Thus, by further design refinement and optimization it is expected that the motor will successfully achieve the target performances.**

Keywords-component; Outer-rotor hybrid excitation flux switching machine; field excitation coil; electric vehicle propulsion; in-wheel drive

I. INTRODUCTION

With increase in world population, demands toward vehicles for personal transportation have increased dramatically in the past decade. However, one of the serious problems associated with ever-increasing use of personal vehicles is the inevitable emissions which contribute to global warming. The conventional internal combustion engine (ICE) vehicles are the main contributors to this problem. According to the report in 2008 [1], seven percent of global carbon dioxide (CO_2) emissions in year 2000 come from vehicles. The global road transport emissions are expected to keep rising proportional with the economic growth and it is projected to double by the year 2050. Because some environmental problems, such as the greenhouse effects are directly related to vehicle emissions, government agencies and organizations have developed more stringent standards for fuel consumption and emissions. Hence, since a decade ago electric, hybrid, and fuel-cell vehicles have attracted increasing attention from vehicle manufactures, governments, and consumers. The Malaysia government through The Ministry of Energy, Green Technology and Water has also looked towards energy saving and reducing CO_2 emissions by creating the relevant policies [2]. Moreover, reviews of the National Automotive Policy (NAP) state that the government will lift the freeze on manufacturing licenses for hybrid and electric vehicles [3]. Meanwhile, PROTON is urged to be more aggressive in competing with foreign vehicle manufacturers especially for hybrid and electric cars where there has been encouraging demand from users on that model due to additional incentives given by the government [4].

Battery-powered electric vehicles (BEVs) seem like an ideal solution to deal with the energy crisis and global warming since they have zero oil consumption and zero emissions. Therefore, Electric Vehicle (EV) is now regarded as an ultimate eco-friendly car and is widely expected to become more popular in the very near future [5]. Presently, research and development efforts have focused on developing advanced powertrains and efficient energy systems. The basic characteristic requirements of an electric motor for EV drive system are: (1) high torque and power density; (2) wide speed range; (3) constant power at high speed; (4) high starting torque for great hill-climbing ability, and high power in speed cruising; (5) high efficiency over wide speed and torque ranges; (6) high reliability and robustness appropriate to environment; (7) intermittent overload ability and acceptable cost; (8) low acoustic noise and low torque ripple; and (9) good voltage regulation over a wide range of speed [6].

M.Z. Ahmad is with Universiti Tun Hussein Onn Malaysia, Johor, 86400 Malaysia (e-mail: zarafi@uthm.edu.my)

978-1-4673-5074-7/13/$31.00 ©2013 IEEE

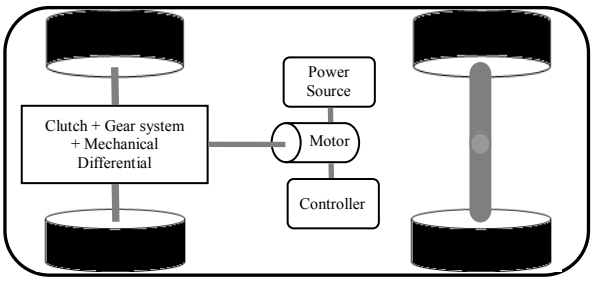

(a)

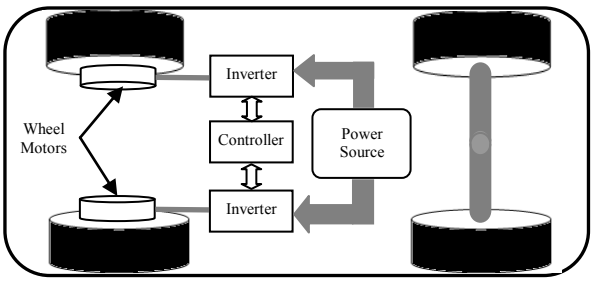

(b)

Fig. 1 EV drivetrain system configurations, (a) Single motor drive, (b) in-wheel motor drive

Generally, there are two main configurations suitable for the electric drivetrain system: (a) centralized motor drive with reduction gears and a differential axle as illustrated in Fig. 1(a), (b) in-wheel direct drives with independent control as shown in Fig. 1(b). Whilst the centralized drive appears to be more popular partly due to its similarity with existing ICE based system. The in-wheel direct drive configuration is gaining popularity as it offers potential superior features. In addition, due to the elimination of mechanical transmission, differential gears and drive belts, the in-wheel direct drivetrain provides quick torque response, higher efficiency, weight reduction, and increased vehicle space.

Permanent magnet synchronous machines (PMSMs) with an outer-rotor have been used as in-wheel direct drive motors for EVs, due to their high torque density, excellent efficiency and overload capability [7]. However, there may be risks of demagnetization and mechanical damage of the rotor's magnet in extreme driving conditions. On the other hand, the switched reluctance motor (SRM) has a very simple and rugged rotor structure without magnets, which makes it particularly robust against mechanical and thermal impacts. On the down side,, SRMs have large torque ripples which make them unsuitable for direct drive. More recently, research and development on permanent magnet flux switching machine (PMFSM) has become more attractive due to several excellent features of physical compactness, robust rotor structure, higher torque and power density, and high efficiency. Thus, the PMFSM inherits selected advantages of both of the PMSM and SRM [8-11]. Since, the outer-rotor configuration is more suitable for direct drive application, the PMFSM with outer-rotor has been proposed only for light EV applications [12-13]. It provides essentially sinusoidal back-electromotive force (emf) and high torque at low speed. However, constant PM flux of PMFSM makes it difficult to control since it requires field weakening flux at high speed conditions. In addition, with rapid increase in the price of rare-earth magnet, the cost of the motor is also becoming higher. Therefore, as one of the candidate that can overcome the problems, a new structure of outer-rotor hybrid excitation flux switching machine (ORHEFSM), which consists of less rare-earth PM and field excitation coil (FEC) on the stator has been proposed by the authors as described in [14]. The proposed motor is simple in structure and potentially can provide much higher torque and power density.

In this paper, design improvement and feasibility studies are conducted on a new 12Slot-10Pole ORHEFSM to achieve the target performances for EV applications. Fig. 2 illustrates the initial design structure of the proposed motor. The original inner-rotor HEFSM performances are described in [10] and the machine composed of 12 PMs and 12 FECs distributed uniformly in the midst of each armature coil.

The rest of the paper consists of the following; Section II will discuss the operating principles of ORHEFSM. Section III describes the design requirements, restrictions, and specifications of the proposed motor. The design improvement methodology is presented in Section IV, while the results and performances of the improved design motor are given in Section V. Finally, Section VI gives a conclusion on this computer design improvement study.

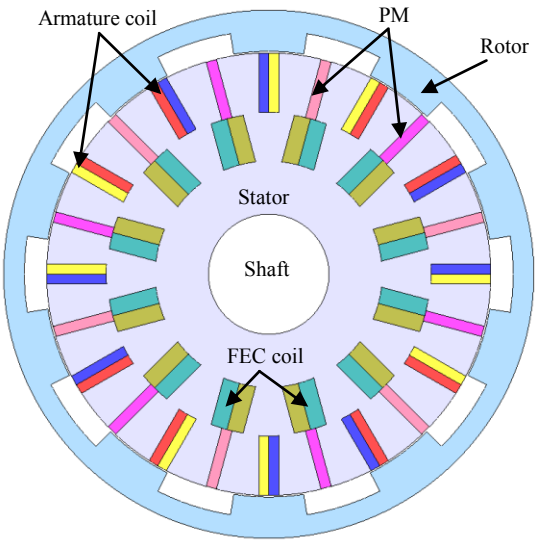

Fig. 2 The initial design structure of ORHEFSM

II. OPERATING PRINCIPLES OF ORHEFSM

The concepts of PMFSM and HEFSM have been introduced in the middle of 1950's [8], and in 2007 [10], respectively. The term "flux switching" is introduced due to the changing of the polarity of the flux linkage by following the motion of salient pole rotor. The flux source of PMFSM is the PM, whereas for the HEFSM, it comes from two flux sources of PM and DC field windings. In both cases, all the active parts are located on the stator with the armature and PM (DC field

winding) allocated to alternate stator teeth. The advantage of this machine is a robust rotor structure that makes it suitable for high speed applications. In addition, the FEC can be used to control the generated flux with variable capabilities. In the proposed ORHEFSM, the possible number of rotor pole and stator slot is defined by

$$N_r = N_s\left(1 \pm \frac{k}{2q}\right) \quad (1)$$

where N_r is the number of rotor poles, N_s is the number of stator slots, k is the integer number, and q is the number of phases. In this study, the selected rotor pole number and stator slot number is 10 and 12, respectively for the three phase motor, $q = 3$.

In this proposed motor, for the motor rotation through 1/10 of a revolution, the flux linkage of armature has one periodic cycle and thus, the frequency of back-emf induced in the armature coil is ten times the mechanical rotational frequency. In general, the relation between the mechanical rotation frequency, f_m and the electrical frequency, f_e for the proposed machine can be expressed by

$$f_e = N_r \cdot f_m \quad (2)$$

where f_e is the electrical frequency, f_m is the mechanical rotation frequency and N_r is the number of rotor poles respectively.

The operating principle of the proposed ORHEFSM is illustrated in Fig. 3. The single piece of rotor that makes the motor more robust similar to SRM is shown in the upper part, while the stator that consists of PMs, FECs, and armature coils are located in the lower part. The PM and FEC are placed between two stator poles to generate excitation fluxes that create the term of "hybrid excitation flux". Figs. 3(a) and (b) demonstrate the flux generated by PM and FEC flow from the stator into the rotor and from the rotor into the stator, respectively, to produce a complete one flux cycle. The combined flux generated by PM and FEC established more excitation fluxes that are required to produce higher torque of the motor. When the rotor moves to the right, the rotor pole goes to the next stator tooth, hence switching the magnitude and polarities of the flux linkage. The flux does not rotate but shifts clockwise and counterclockwise in direction with each armature current reversal. According to Figs. 3(c) and (d), only the PM flux flows from the stator into the rotor and from the rotor into the stator, respectively, while the FEC flux is only circulating on its particular winding slots. This condition establishs less excitation flux and generates less torque.

III. Design Requirements, Restrictions and Specifications

The design requirements, restrictions and specifications for the proposed ORHEFSM are similar with interior permanent magnet synchronous motor (IPMSM) employed in LEXUS RX400h and listed in Table I. The target maximum torque and power are set to be more than 333 Nm and 123 kW, respectively. The PM weight is set to 1.0 kg, which less by 0.1 kg compared with the PM used in inner rotor HEFSM. The corresponding electrical restrictions to the inverter such as maximum DC bus voltage and maximum inverter current are set to 650 V and 360 A_{rms}, respectively, while the limit of both armature current density, J_a and FEC current density, J_e is set to 30 A/mm^2. The proposed motor has very simple structure where all the components shape are in rectangle form and all coils are in concentrated winding. In addition, its offers non-overlap winding between the FEC and armature coil that makes shorter end winding and can contribute to reduce copper loss effect. The target weight of the proposed motor is set to be at least similar as inner rotor HEFSM which is 35 kg. Therefore, the proposed motor is expected to achieve the maximum power and torque density of 9.5 Nm/kg and 3.5 kW/kg, respectively.

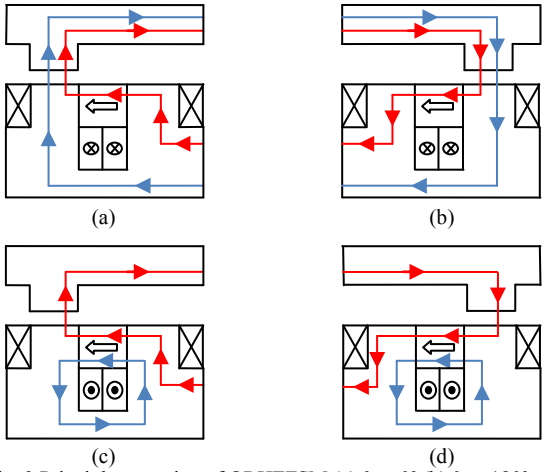

Fig. 3 Principle operation of ORHEFSM (a) $\theta_e = 0°$ (b) $\theta_e = 180°$ more excitation, (c) $\theta_e = 0°$ (b) $\theta_e = 180°$ less excitation

TABLE I. Outer-Rotor HEFSSM Design Restrictions and Specifications

Descriptions	Inner rotor HEFSM	Outer-rotor HEFSM
Max. DC-bus voltage inverter (V)	650	650
Max. inverter current (A_{rms})	360	360
Max. current density in armature coil, J_a (A_{rms}/mm^2)	30	30
Max. current density in FEC, J_e (A/mm^2)	30	30
Motor radius (mm)	132	132
Motor stack length (mm)	70	70
Shaft/Inner motor radius (mm)	30	30
Air gap length (mm)	0.8	0.8
PM weight (kg)	1.1	1.0
Maximum torque (Nm)	333	>333
Maximum power (kW)	123	>123

The commercial FEA package, JMAG-Designer ver.12.0, released by Japan Research Institute is used as 2D-FEA solver in this design. The material used for PM is NEOMAX 35AH with residual flux density and coercive force at 20 ° are 1.2T and 932 kA/m, respectively. Whereas for the stator and rotor body, the material used is electrical steel, 35H210.

Initially, the 30° mechanical angle of stator yoke is designed with the following assumptions; (i) The inner radius is set to 30 mm for the motor's shaft while the outer radius is set to 110.6 mm, making the stator depth of 80.6 mm which is

61% of 132 mm motor radius and within the range of general machine split ratio, (ii) The PM volume is set to 1.0 kg, which is less 0.1 kg compared with the PM used in IPMSM. The reason is to reduce the PM cost due to the increasing price of PM since 2011, (iii) By expecting that the higher of the PM depth will give more flux to flow and increase the motor performances, therefore the PM depth is set to 29.7 mm which is approximately one third of stator depth. However, demagnetization effect needs to be taken into consideration when higher PM depth is applied especially at the edge of the PM, (iv) The FEC slot area is set to 197.01 mm^2 to give a maximum current density, J_e of 30 A/mm^2 with 44 turns of FEC winding. The FEC slot depth is less than the PM depth to give an appropriate distance between two FEC slots area for the flux to flow in this area, (v) The depth of armature slot area is set similar to the PM depth in order to avoid overlapping between armature coil winding and FEC winding. Therefore, it is expected that the motor will use shorter coil end winding and so reduces copper loss effect.

Besides that, the initial for 36º mechanical angle of rotor iron is designed with the following assumptions; (i) The air gap is set similar as the IPMSM which is 0.8 mm, hence the inner rotor radius becomes 111.4 mm and this gives a rotor depth of 20.6 mm, (ii) The rotor pole depth is set to 10.3 mm which is half of the rotor iron depth to allow the flux flow easily through the outer rotor pitch, (iii) The rotor pole arc width is set to be similar with the rotor pole gap to allow optimal flux flows into the rotor pitch.

IV. Improved Design Methology

In this design improvement study, the motor parameters are divided into two groups, namely, those related to stator iron core and rotor iron core. On the stator iron core, it is subdivided into three components which are the PM shape, FEC slot shape, and armature slot shape. The rotor parameters involved are the inner rotor radius (D_1), rotor pole depth (D_2), and rotor pole arc width (D_3). The distance between airgap and PM is (D_4). The PM slot shape parameters are the PM depth (D_5), and the permanent magnet width (D_6), while for the FEC slot parameters are FEC slot depth and FEC slot width, (D_7) and (D_8) respectively. Finally, the armature coil parameters are armature coil slot depth (D_9) and the armature coil slot width (D_{10}). The motor design parameters, from D_1 to D_{10} are demonstrated in Fig. 4. Based on the motor parameters identified, the deterministic design optimization method is used and implemented using 2-D FEA solver to obtain the optimal performances of the proposed motor. In summary, the motor parameters D_1 to D_{10} are changed repeatedly until the target performances of torque and power are achieved. In this study, the initial design and improved design parameters of the proposed ORHEFSM are depicted in Table II. The improved design structure of ORHEFSM is illustrated in Fig. 5. In this design improvement, the simple structure of the proposed motor is retained and overlap between armature coil and FEC coil windings avoided.

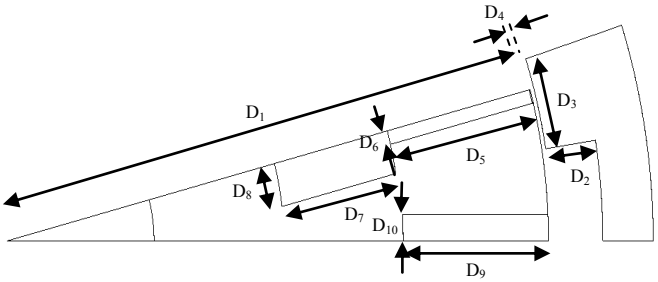

Fig. 4 Design parameters defined as $D_1 - D_{10}$

TABLE II. The Design Parameters for The Proposed ORHEFSM

Parameter	Description	Initial	Improved
D_1	Rotor inner radius (mm)	110.6	108.4
D_2	Rotor pole depth (mm)	10.3	12.3
D_3	Rotor pole arc width (º)	9	13
D_4	Distance between airgap and PM (mm)	0.2	0
D_5	PM depth (mm)	30	20
D_6	PM width (mm)	2.63	3.95
D_7	FEC slot depth (mm)	23.88	40.60
D_8	FEC slot width (mm)	8.25	5.03
D_9	Armature coil slot depth (mm)	29.7	17.2
D_{10}	Armature coil slot width (mm)	4.95	8.14

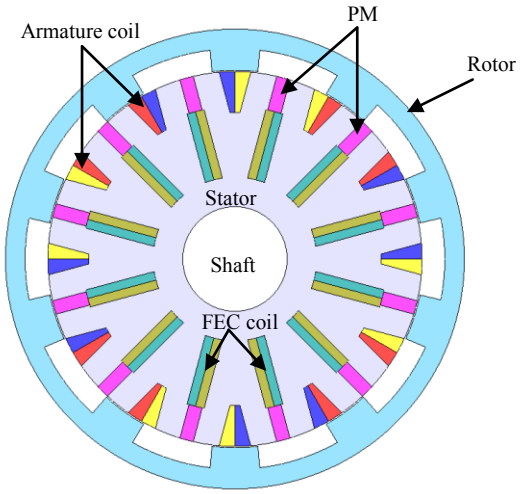

Fig. 5 Improved design structure of ORHEFSM

V. Results and Performances of the Improved Design

A. *Open circuit analysis*

Initially, the magnetic flux linkage in open circuit condition of the proposed motor is investigated based on 2D-FEA. The flux linkage of the initial and improved design at various condition of J_e is plotted in Fig. 6 and Fig. 7, respectively. From these two figures, it is clearly demonstrated that the magnitude of flux linkage of the improved design at

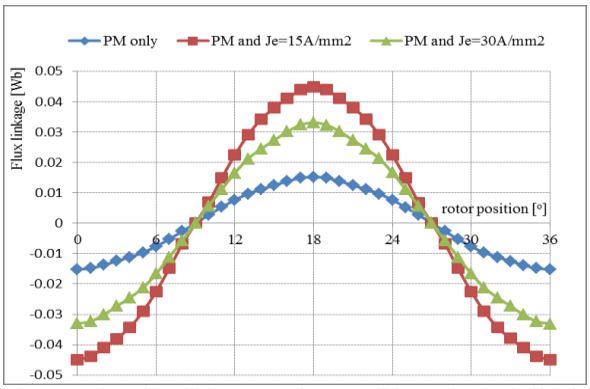

Fig. 6 U-phase flux linkage at various conditions of Je for initial design motor

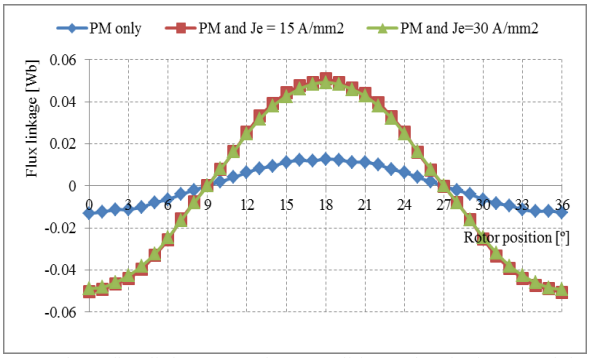

Fig. 7 U-phase flux linkage at various conditions of Je for improved design motor

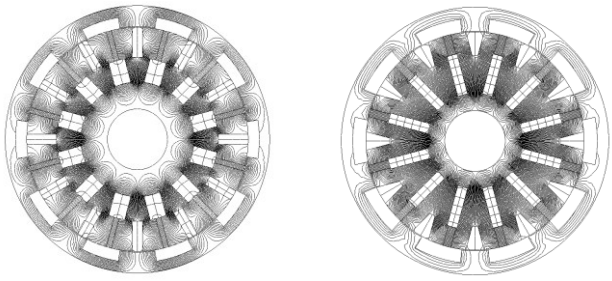

(a) (b)

Fig. 8 Flux path of PM in open circuit condition (a) Initial design (b) Improved design

maximum J_e has increased from 0.03 Wb to 0.05 Wb. Hence, it has the ability to increase the performances of the motor.

Besides that, the field distribution for PM of initial design and improved design ORHEFSM are also investigated and the results obtained are shown in Fig. 8. From the diagram, it shows that for initial design 50 % of PM flux flows to the rotor causing higher generated induce voltage, while for the improved design, there is a great reduction of flux flow to the rotor which is approximately 10 % of generated flux. Consequently, it provides less cogging torque and reduces the amplitude of back-emf at open circuit condition. The comparison of back-emf of initial and improved design ORHEFSM at the speed of 3000 r/min is illustrated in Fig. 9. It is clearly shown that the amplitude of back-emf for the improved design motor has significantly been reduced from 82.44 V to 70.78 V, which is approximately 14% reduction. In addition, the back-emf of the improved designed motor looks more sinusoidal compared with the initial design motor.

Furthermore, the cogging torque of the improved design ORHEFSM compared with the initial design is exemplified in Fig. 10. From the graph, the improved design motor shows great reduction in peak-to-peak cogging torque ripple where it has reduced 76.7% from 10.2 Nm to 3.6 Nm. Therefore, it is expected that the motor has the potential to be applied for high speed applications.

B. Load Analysis

In load analysis, the torque versus FEC current density at maximum J_a and the average torque of the initial and improved design is compared and plotted as depicted in Fig. 11 and Fig. 12, respectively. The average maximum torque obtained for the initial design is 205.6 Nm, whilst the improved design ORHEFSM is 271.5 Nm. It is shown that the improved design motor has produced higher torque with 32% improvement compared to initial design motor and has achieved 81.5 % from the target value. The torque obtained at various conditions of J_e and J_a for improved design ORHEFSM are also analyzed and plotted as shown in Fig. 13. From the diagram, when J_a is set at maximum of 30 A_{rms}/mm^2, the torque keeps increasing as J_e is increased from 0 A/mm^2 to 30 A/mm^2. Whereas, when J_a is set between 10 A_{rms}/mm^2 to 25 A_{rms}/mm^2, the output torque is maintained constant for J_e greater than 25 A/mm^2. This phenomenon is due to the flux saturation effect and an investigation on magnetic flux distribution is required to overcome the problem.

Consequently, with the improvement of the maximum torque of the improved design ORHEFSM, the maximum power also has been increased and obviously it has achieved beyond the target value. Previously, for the initial design motor the maximum power achieved was 70.4 kW, while for the improved design motor, it has increased dramatically to 143.6 kW, since the target maximum power is only 123 kW. Although, the target performance for the maximum torque was not achieved, further design refinement and optimization will be conducted in future and it is expected the target performance will be achieved.

VI. CONCLUSION

In this paper, design improvement studies of 12Slot-10Pole ORHEFSM for in-wheel drive EV applications have been presented. The simulated performances of the proposed motor has achieved 81.5% from the target value of maximum torque, whilst for the maximum power has achieved beyond the target performances. Thus, it is expected that the target performance for the maximum torque can be achieved by further design refinement and optimization in future.

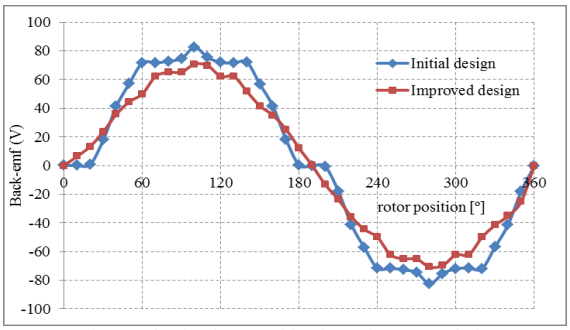

Fig. 9 The fundamental back-emf at 3000 r/min

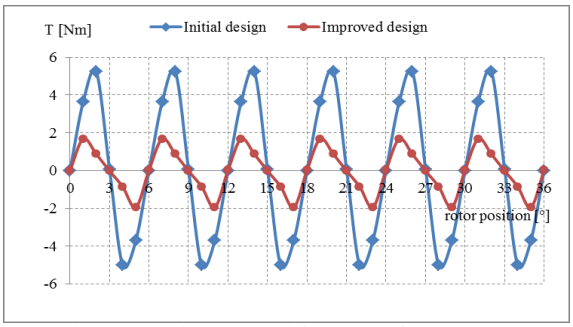

Fig. 10 Cogging torque of the proposed ORHEFSM

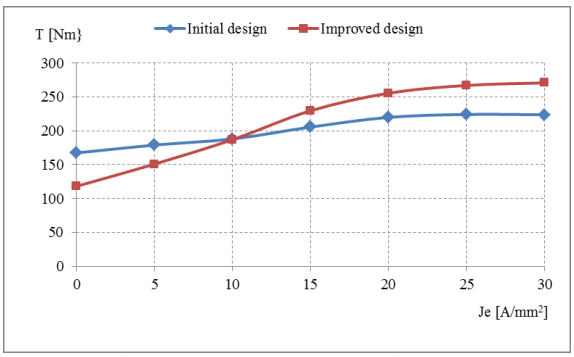

Fig. 11 Torque versus J_e at maximum J_a

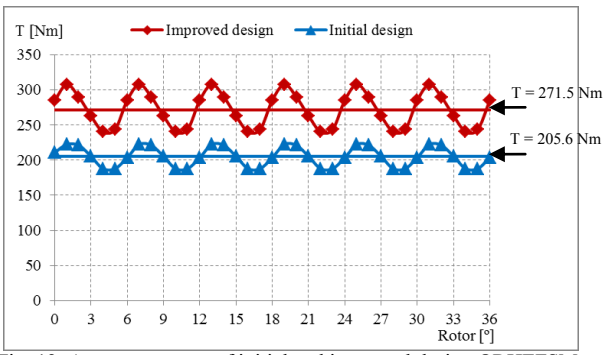

Fig. 12 Avaerage torque of initial and improved design ORHEFSM

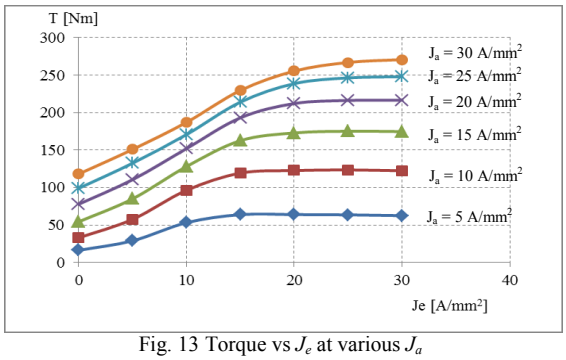

Fig. 13 Torque vs J_e at various J_a

REFERENCES

[1] J. King, *The King Review of low-carbon cars - Part II: recommendations for action*, March 2008. Available at: www.hm-treasury.gov.uk/king

[2] National Green Technology Policy [Online] Available at: http://www.kettha.gov.my/en/content/policies-acts-guidelines-1 (Accessed on Jan 2013)

[3] Review of National Automotive Policy [Online] Available at: http://www.pekema.org.my (Accessed on Jan 2013)

[4] Berita Harian online, Ekonomi "PROTON digesa lebih agresif" 14 Jan 2013 (Accessed on 16 Jan 2013)

[5] IEA-HEV Outlook, International Energy Agency Implementing Agreement on Hybrid and Electric Vehicles, "Outlook for hybrid and electric vehicles," 2008 [Online] Available: http://www.ieahev.org/pdfs/iahev_ outlook_2008.pdf

[6] W. Xu, J. Zhu, Y. Guo, S. Wang, Y. Wang, and Z. Shi, "Survey on electrical machines in electrical vehicles," *2009 International Conference on Applied Superconductivity and Electromagnetic Devices*, no. c, pp. 167–170, Sep. 2009.

[7] W. Fei, P. Luk, and K. Jinupun, "A New Axial flux magnet segmented- armature-torus machine for in-wheel direct drive applications," IEEE Power Electronics Specialist Conference, pp. 2197-2202, 2008.

[8] S. E. Rauch and L. J. Johnson, "Design principles of flux switch altenators," AIEE Trans., vol 74III, no. 12, pp. 1261-1269, 1955.

[9] Y. Chen, S. Chen, Z.Q. Zhu, D. Howe, and Y.Y. Ye, "Starting torque of single phase flux switching permanent magnet motors," IEEE Trans. Magn., vol 42, no. 10, pp. 3416-3418, 2006.

[10] E. Hoang, M. Lecrivain, and M. Gabsi, "A New Structure of a Switching Flux Synchronous Polyphased Machine," in *European Conference on Power Electronics and Applications*, no. 33, pp. 1–8, 2007.

[11] Y. Amara, E. Hoang, M. Gabsi, and M. Lecrivain, "Design and comparison of different flux-switching synchronous machines for an aircraft oil breather application," Euro. Trans Electr. Power, no. 15, pp. 497-511,2005.

[12] W. Fei, P. Chi, K. Luk and J. S. Y. Wang, "A Novel Outer-Rotor Permanent-Magnet Flux-Switching Machine for Urban Electric Vehicle Propulsion," in *3rd International Conference on Power Electronics Systems and Applications (PESA)*, pp. 1–6, 2009.

[13] W. Fei, P. Chi, K. Luk, S. Member, J. X. Shen, Y. Wang, and M. Jin, "A Novel Permanent-Magnet Flux Switching Machine With an Outer-Rotor Configuration for In-Wheel Light Traction Applications," *IEEE Transactions on Industry Applications*, vol. 48, no. 5, pp. 1496–1506, 2012

[14] M.Z. Ahmad, E. Sulaiman, Z.A. Haron, and T. Kosaka, "Preliminary Studies on a New Outer-Rotor Permanent Magnet Flux Switching Machine with Hybrid Excitation Flux for Direct Drive EV Applications", IEEE Int. Power and Energy Conference (PECON2012), pp. 928-933, Dec 2012.